

# High Isolation UWB-MIMO Compact Micro-strip Antenna

Ze-Lin Song, Zhao-Jun Zhu, and Lu Cao

Institute of Applied Physics  
University of Electronic Science and Technology of China, Chengdu, 610054, China  
Songzelin0208@126.com, uestc98@163.com, cl\_stella@163.com

**Abstract** — A compact four-unit ultra-wideband multiple-input multiple-output (UWB-MIMO) antenna with very high isolation, dual polarization, notched structure, and achieving dual-state operation, along with smaller volume, is proposed in this paper. The proposed MIMO antenna element consists of two parts: the front patch composed of four symmetrical trapezoidal radiating elements and feeder, and the back composed of a rectangular annular ground. The offset of antenna operating frequency band is achieved by adjusting the rectangular patch in the middle of the back side, and by introducing an X-shaped metal narrow strip on the top side and an X-shaped slit on the bottom side to improve the isolation in the single port feeding state of antenna. Finally, the dimension of the antenna is  $32 \times 32 \text{mm}^2$ . Under the frequency from 3.1 GHz to 10.6 GHz, the isolation in the condition of differential mode can below -30 dB, which is very high, and also can work in the single port inputting state, showing a dual mode operation. In addition, a trapezoidal slit is introduced to obtain a notch structure. The measured results and simulation results are consistent.

**Index Terms** — Dual polarization, dual-state operation, micro-strip, notch band, UWB-MIMO antenna.

## I. INTRODUCTION

Multi-input multiple-output (MIMO) technology has the advantage of regarding the multi-path radio channel with the transmitter and receiver as a whole to optimize, so as to achieve high communication capacity and spectrum utilization rate. MIMO technology is a kind of near-optimal diversity to the spatial and temporal congregation and technique of interference cancellation, making it receive more and more attention in recent years. The U.S. Federal Communications Commission has released a 3.1-10.6 GHz bandwidth as Ultra-wideband (UWB) in 2002 [1], a new type of wireless Communication technology, which has many advantages including wide bandwidth, high-data-rate wireless transmission, high capacity, and low-power consumption. The combination of UWB technology with MIMO technology, the use of space multipath, parallel transmission of multiple signals,

can obtain obvious multiplexing gain and diversity gain, and achieve a stable signal transmission in distance. Isolation is one of the most important performance indicators of MIMO antennas, achieving high isolation and small size is also a challenge. Several UWB-MIMO antennas are reported recently [2-4]. But, especially for the compact UWB antenna, their components is very difficult to reduce, so compared with narrowband antennas' mutual coupling, which is difficult to realize the isolation degree is higher than 20 dB [4]. Two differential feed antenna reported recently also has high isolation [5, 6], while they have a common problem, both antennas are only able to operate in differential mode, and cannot work in others condition. The antenna proposed in this paper has two pairs of ports and symmetrical structure, work well with a very high degree of isolation in the differential mode excitation state, but when working in the single port feeding state, it can also work normally, thus making the antenna have a wider range of applications and the volume on the basis of the original reduced very much. Additionally, in order to facilitate the application, attaching the trapezoidal gap to the antenna patch can achieve the notched structure [7-9], can perfectly cover 5.2 and 5.8 GHz WLAN signal. The details of the antenna design and simulation, measurement results are as follows.

## II. UWB-MIMO ANTENNA DESIGN

As shown in Fig. 1, the four radiation units of the Antenna-A are placed tightly and symmetrically on the top side of the substrate to reduce the size of antenna. Each radiating element consists of a trapezoidal patch and a feeder of the same size. In the state of differential mode inputting, two pairs of differential ports are orthogonal to each other. In theory, infinite isolation can be achieved under differential input conditions, furthermore dual polarization can be achieved. The back of the substrate consists of a rectangular ring ground and a rectangular patch in the middle, and the four units of the antenna share the rectangular radiation gap on the back, and the central rectangular patch and the four rectangular holes in the middle of the annular ground are used to adjust the left and right offset of the antenna band.

In order to make the antenna work properly in the single port feeding mode, introduction of the X-shaped metal narrow strip on the top side and the X-shaped slit on the bottom side can improve the isolation in single port feeding state of antenna. The final parameters for antenna are listed in Table 1.

Table 1: Parameter of the Antenna-A

Parameter	L	h	Wf	Lc	Wc
Value (mm)	32	0.508	1	2	3
Parameter	Lf	L1	L2	W1	Li
Value (mm)	2.9	7.7	9.5	2	26.1
Parameter	L2	Wp	Wg		
Value (mm)	9	0.1	0.1		

The total size of the antenna is just  $32 \times 32mm^2$ , reduced very much compared with others, much smaller than the recent published antennas.

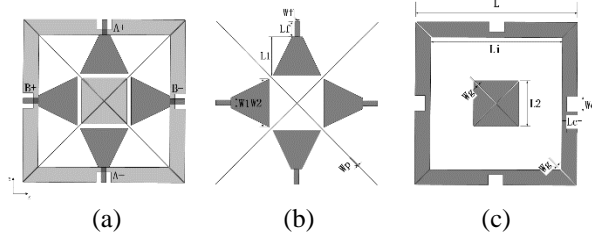


Fig. 1. Configuration of the proposed Antenna-A: (a) whole geometric structure, (b) the top view, and (c) the bottom view.

For the differential mode, the grounding line is symmetrical along two differential ports. Under differential excitation mode, the Port-A and Port-B of the MIMO antenna are symmetrical along the X-axis and Y-axis. Figure 2 shows the electric field distribution in the low frequency, intermediate frequency and high frequency of the Antenna-A part when only the Port-A of the Antenna-A is differential inputted. It is obvious that the virtual ac of Port-A is distributed along the Y-axis in the entire frequency band, while Port-B is arranged on the virtual ac ground of Port-A. The minimum value of current on virtual communication is zero. Because the Port-B is symmetrical in the same, so the Port-A is situated on the ac ground of the Port-B, so either the Port-A or Port-B is excited, the other has no signal. In this way, the theoretical differential isolation between Port-A and Port-B is not limited.

With reference to the [10], the differential coupling between the two differential Ports A and B can be calculated by:

$$S_{ba} = S_{11} - S_{41} - S_{32} + S_{42}, \quad (1)$$

$$S_{ba} = S_{13} - S_{14} - S_{23} + S_{24}. \quad (2)$$

Since the antenna is symmetrical, then  $S_{ab}$  should theoretically equal to  $S_{ba}$ . Figure 3 shows the simulated

and measured differential coupling between the two adjacent ports of the Antenna-A. Because the result is obtained by calculation, the machining error and measurement environment error are further magnified in the calculation, so the measurement result and the simulation result will produce some error. But the manufactured antennas still achieve a very high differential isolation at up to 30 dB over the entire frequency band.

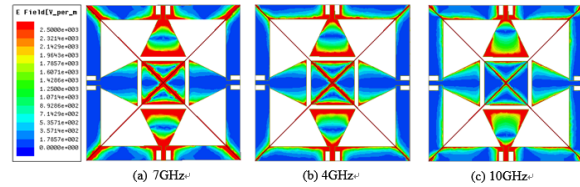


Fig. 2. The distribution of E-field of Antenna-A at different frequencies with only differential Port-A excited.

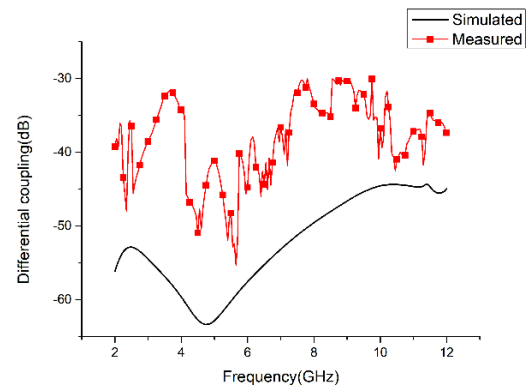


Fig. 3. The simulated and measured differential coupling between Port-A and Port-B.

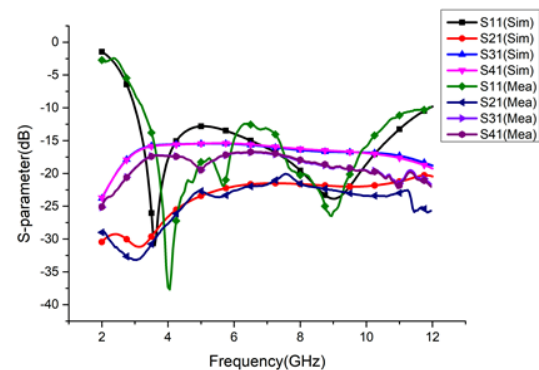


Fig. 4. The Simulated and measured S-parameter of the Antenna-A in the single port feeding state.

Just as mentioned earlier, the isolation of two recently reported differential mode feed antennas is relatively high, but they cannot work well under single

port excitation conditions, which will undoubtedly limit the condition of usage, bringing inconvenience to users. The antenna mentioned in this paper not only have an ultra-high isolation of -45 dB below in the differential feeding conditions, but also can work in the single port feeding conditions. The X-shaped metal narrow strip on the top and the X-shaped slit on the bottom are introduced to improve the isolation in single port feeding state enable the antenna to operate normally. The single port feeding state of the antenna is shown in Fig. 4. This greatly facilitate convenience to the customer, and also expand the performance of antenna.

**III. NOTCHED STRUCTURE**

In order to avoid interfering with the wireless local area network (WLAN) system (5.2 GHz, 5.8 GHz) and facilitate people’s using, a half-wavelength slit resonator was introduced, Antenna-B shown in Fig. 5, to achieve a 4.5-6.3 GHz notch structure. The sizes of slits and antennas are shown in Table 2.

Table 2: Parameter of the Antenna-B

Parameter	L	h	Wf	Lc	Wc
Value (mm)	32	0.508	1.3	1.8	2.2
Parameter	Lf	L1	L2	W1	Li
Value (mm)	2.8	8	9.8	1.5	27
Parameter	L2	Wp	Wg	Ls1	S
Value (mm)	9.8	0.1	0.1	4.5	0.1
Parameter	W2	Ws1	hs	Ws2	
Value (mm)	8.1	2.34	2	5.2	

At 5.2 GHz and 5.8 GHz, the current mainly flows along the half-wavelength slit etched in the trapezoidal patch which leads to the impedance matching of the antenna being deteriorating seriously. Consequently, the antenna hardly radiates at these frequencies, the band-notched characteristic is obtained.

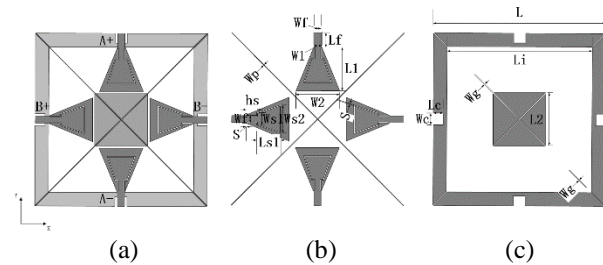


Fig. 5. Configuration of the proposed Antenna-B: (a) whole geometric structure, (b) the top view, and (c) the bottom view.

**IV. RESULT AND DISCUSSION**

As shown in Fig. 6, the proposed Antenna-A and Antenna-B are made of a substrate with relative permittivity of 2.2 and thickness of 0.508 mm. Especially,

the proposed antenna is much smaller than the previously reported UWB antennas. The comparison is presented in Table 3.

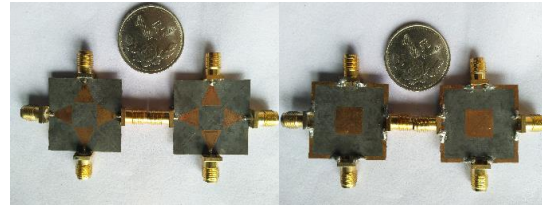


Fig. 6. Photograph of the fabricated Antenna-A and Antenna-B.

Table 3: Comparison of the related UWB-MIMO antennas

Antenna	Measured Isolation (dB)	Notched Bands (GHz)	Electrical Size ( $\lambda_g * \lambda_g$ )
[2]	-15	No	1.87*1.87
[3]	-15	5.5	2.06*2.06
[5]	-35	5.8/7.4	1.03*1.03
[6]	-13	5.2/5.8	0.43*0.43
This work	-30	5.2/5.8	0.47*0.47

Referring to [10], the odd mode reflection coefficient can be calculated by:

$$S_{dd} = (S_{11} - S_{12} + S_{22} - S_{21})/2. \quad (3)$$

Figure 7 is the odd mode reflection coefficient of the simulation and measurement of the two antennas. We can clearly see that the simulation results of Antenna-A and Antenna-B are both below -10 dB in the 3.1GHz-10.6 GHz, which can perfectly cover the ultra-broadband frequency band, as well as Antenna-B notch-band (4.5– 6.3 GHz) and with a measured -10 dB impedance bandwidth from 3.6 to 10.6 GHz, as well as notch-band (4.9–6.2 GHz); although the measured results and simulated results have some errors, but based on processing and environment of measurement impact, these errors within the acceptable range. In general, the measurement results and simulation results are consistent.

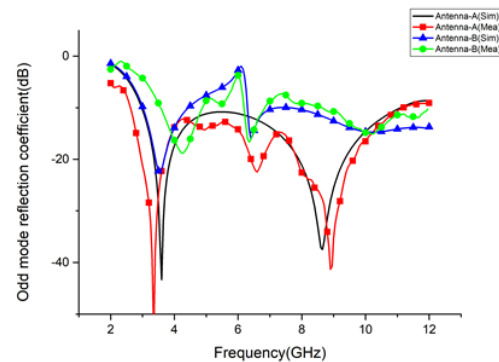


Fig. 7. Simulated and measured odd mode reflection coefficients of Antenna-A and Antenna-B.

The radiation patterns of Antenna-B at 4 GHz, 7 GHz and 10 GHz is shown in Fig. 8. It can be seen that the proposed Antenna-B represents an omnidirectional radiation pattern in the H-plane, and the radiation pattern maintains the shape of the E-plane shown in Fig. 7 in the whole frequency band. Because of the normalized cross-polarization components in H-plane and E-plane simulations are all lower than -40 dB, the normalized cross-polarization components in H-plane and E-plane simulations are all lower than -40 dB.

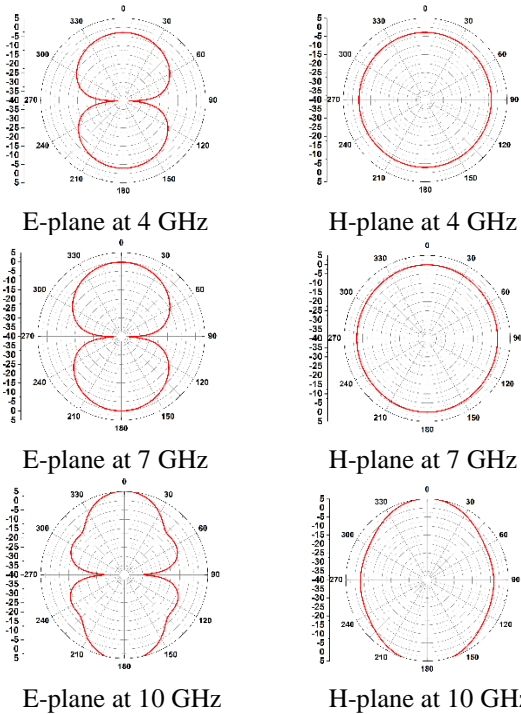


Fig. 8. Normalized radiation patterns of the proposed Antenna-B when Port-A is excited and Port-B is terminated with 50Ω load.

The Envelope correlation coefficient (ECC) is an important parameter to measure the performance of MIMO system, which can be calculated using the radiation pattern [11] or the S-parameter. Now, we use the S parameter to calculate the ECC by:

$$ECC = \frac{|S_{11}^* S_{12} + S_{21}^* S_{22}|^2}{(1 - |S_{11}|^2 - |S_{21}|^2)(1 - |S_{22}|^2 - |S_{12}|^2)}. \quad (4)$$

In real life, the mobile system requirements for the ECC is less than 0.5. As can be seen from Fig. 9, since the degree of isolation between the adjacent differential ports is very high, we can calculate the ECC of the MIMO Antenna-B is less than 0.0001 in non-notch band. For the mobile system, the antenna is proposed in this paper is excellent.

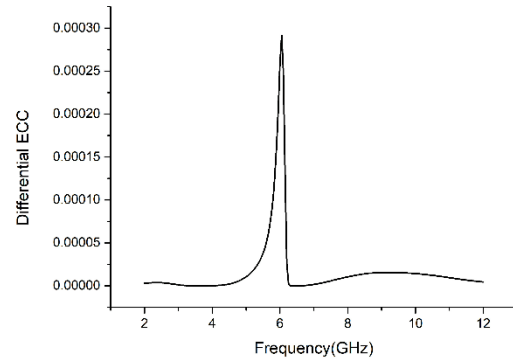


Fig. 9. Calculated ECC of the proposed Antenna-B.

## V. CONCLUSION

This paper introduces a compact four-unit UWB-MIMO antenna that enables dual-state operation and is much smaller. Dual orthogonal polarization and pretty high differential isolation can be obtained by arranging two pairs of differential ports in the virtual ac ground lines of each other. An X-shaped metal narrow strip on the top side and an X-shaped slit on the bottom side were introduced to improve the isolation in the single port feeding state of antenna. To realize notch-band characteristic, the half-wavelength slits were introduced. The measurement results and simulation results are consistent, so we can conclude that the proposed antenna is suitable for UWB communication systems.

## ACKNOWLEDGEMENT

This work is supported by “National Natural Science Foundation of China (Grant No. 61101042)”.

## REFERENCES

- [1] Federal Communications Commission, “First report and order in the matter of revision of part 15 of the commission’s rules regarding ultra-wideband transmission systems,” ET-Docket 98-153, Apr. 22, 2002.
- [2] E. A. Daviu, M. Gallo, B. B. Clemente, and M. F. Bataller, “Ultra-wideband slot ring antenna for diversity applications,” *Electron Lett.*, vol. 46, pp. 478-480, 2010.
- [3] P. Gao, S. He, X. B. Wei, Z. Q. Xu, N. Wang, and Y. Zheng, “Compact printed UWB diversity slot antenna with 5.5-GHz band-notched characteristics,” *IEEE Antennas Wireless Propag. Lett.*, vol. 13, pp. 237-240, 2014.
- [4] J. F. Li, Q. X. Chu, Z. H. Li, and X. X. Xia, “Compact dual bandnotched UWB MIMO antenna with high isolation,” *IEEE Trans. Antennas Propag.*, vol. 61, pp. 4759-4766, 2013.
- [5] W. A. Li, Z. H. Tu, and Q. X. Chu, “Compact, high isolation and dual-polarized differential dual-

- [6] notched UWB-MIMO slot antenna,” *IEEE Microw. Opt. Technol. Lett.*, vol. 57, no. 11, pp. 2609-2614, Nov. 2015.
- [7] Y. Y. Liu and Z. H. Tu, “Compact differential band-notched stepped-slot UWB-MIMO antenna with common-mode suppression,” *[J]. IEEE Antennas & Wireless Propagation Letters*, 16 (99):1-1, 2017.
- [8] J. R. Kelly, P. S. Hall, and P. Gardner, “Band-notched UWB antenna incorporating a microstrip open-loop resonator,” *IEEE Trans. Antennas Propag.*, vol. 59, no. 8, pp. 3045-3048, Aug. 2011.
- [9] Y. Sung, “Triple band-notched UWB planar monopole antenna using a modified H-Shaped resonator,” *IEEE Trans. Antennas Propag.*, vol. 61, no. 2, pp. 953-957, Feb. 2013.
- [10] T. G. Ma and J. W. Tsai, “Band-rejected ultra-wideband planar monopole antenna with high frequency selectivity and controllable bandwidth using inductively coupled resonator pairs,” *IEEE Trans. Antennas Propag.*, vol. 58, no. 8, pp. 2747-2752, Aug. 2010.
- [11] Q. Xue, S. W. Liao, and J. H. Xu, “A differentially-driven dual-polarized magneto-electric dipole antenna,” *IEEE Trans. Antennas Propag.*, vol. 61, pp. 425-430, 2013.
- [12] R. G. Vaughan and J. B. Andersen, “Antenna diversity in mobile communications,” *IEEE Trans. Veh. Technol.*, vol. 36, pp. 149-172, 1987.



**Zelin Song** was born in Tianjin city, China, in 1991. He received the B.S. degree in Physics from the UESTC in 2015, and is working toward the M.D. degree in the UESTC. He research interests include the design of microwave and millimeter-wave circuits.



**Zhaojun Zhu** was born in Sichuan, China, in 1978. He received the B.S. degree and the Ph.D. degree in Physical Electronics in UESTC, Chengdu, in 2002 and 2007 respectively. Since 2012, he has been an Associate Professor with the UESTC. His research interests include the design of microwave and millimeter-wave circuits.



**Lu Cao** was born in Jiangxi Province, China, in 1993. She received the B.S. degree in Physics from Gannan Normal University, in 2015, and is currently working toward the M.D. degree in UESTC. Her research interests include the design of microwave and millimeter-wave circuits.